Available online at www.sciencedirect.com
ScienceDirect
Remote Sensing of Environment 112 (2008) 2326–2340
Remote Sensing of Environment
www.elsevier.com/locate/rse

Spatially explicit characterization of boreal forest gap dynamics using multi-temporal lidar data

Udayalakshmi Vepakomma [a], Benoit St-Onge [b,*], Daniel Kneeshaw [c]

[a] Institut des sciences de l'environnement, Université du Québec à Montréal, C.P. 8888 succ. Centre-ville, Montréal, Canada H3C 3P8
[b] Département de géographie, Université du Québec à Montréal, C.P. 8888 succ. Centre-ville, Montréal, Canada H3C 3P8
[c] Département des sciences biologiques, Université du Québec à Montréal, C.P. 8888 succ. Centre-ville, Montréal, Canada H3C 3P8

Received 14 June 2007; received in revised form 10 September 2007; accepted 27 October 2007

Abstract

Understanding a disturbance regime such as gap dynamics requires that we study its spatial and temporal characteristics. However, it is still difficult to observe and measure canopy gaps extensively in both space and time using field measurements or bi-dimensional remote sensing images, particularly in open and patchy boreal forests. In this study, we investigated the feasibility of using small footprint lidar to map boreal canopy gaps of sizes ranging from a few square meters to several hectares. Two co-registered canopy height models (CHMs) of optimal resolution were created from lidar datasets acquired respectively in 1998 and 2003. Canopy gaps were automatically delineated using an object-based technique with an accuracy of 96%. Further, combinatorics was applied on the two CHMs and the delineated gaps to provide information on the area of old and new gaps, gap expansions, new random gap openings, gap closure due to lateral growth of adjacent vegetation or due to vertical growth of regeneration. The results obtained establish lidar as an excellent tool for rapidly acquiring detailed and spatially extensive short-term dynamics of canopy gaps.

Keywords: Gap; Lidar; Forest dynamics; Boreal forests

1. Introduction

Research in various forest ecosystems has demonstrated that in the absence of large-scale disturbances like fire and insect infestation, forest canopy dynamics in mature and old-growth forests are driven by local gap dynamics (Kneeshaw & Bergeron, 1998; Runkle, 1981). Small, partial disturbances due to snapping, blow down, insects or pathogens create canopy openings termed "gaps". They increase space and site resource availability and eventually are closed by tree regeneration or lateral growth of surrounding vegetation determining a new canopy structure (Bongers, 2001; McCarthy, 2001). Gaps are important for certain tree species to attain canopy status in mature forests (Denslow & Spies, 1990). They play an important role in maintaining species heterogeneity and in driving successional dynamics (Frelich & Reich, 1995; Payette et al., 1990). Hence the accurate characterization of these disturbances will have a direct impact not only on our perception of ecological processes but also on the quality of management practices when gap dynamics are adopted as a template for ecosystem based management.

Gaps are characterized by their size, shape, rates at which they open and close and the causes of such events (Denslow & Spies, 1990; Runkle, 1991). Although traditional ground (Battles et al., 1995; Lertzman & Krebs, 1991; Kneeshaw & Bergeron, 1998; Runkle, 1991) and conventional remote sensing based methods (D'Aoust et al., 2004; Foody et al., 2003; Fox et al., 2000; Jackson et al., 2000) have provided useful results on tree replacement and resource heterogeneity, they are limited in their ability to represent spatial patterns and temporal dynamics. In fact, most research has been at the scale of only a few gaps, restricted to evaluating current forest conditions, or has been based on space-for-time substitution. Retrospective studies through long-term installations of permanent sample plots or

* Corresponding author. Tel.: +1 514 987 3000x0280; fax: +1 514 987 6784.
E-mail address: st-onge.benoit@uqam.ca (B. St-Onge).

0034-4257/$ - see front matter © 2007 Elsevier Inc. All rights reserved.
doi:10.1016/j.rse.2007.10.001

through dendrochronology are costly and time consuming, while simulation models use arbitrary areal units, and often include random initial conditions. Moreover, conventional remote sensing based methods (aerial photography, bi-dimensional analysis of space images) have been criticized for their inadequacy in gap identification due to illumination conditions and spectral inseparability (Koukoulas & Blackburn, 2004; Tanaka & Nakashizuka, 1997).

Characterizing and understanding the pattern and dynamics of these ecological processes rely on the study of the horizontal and vertical arrangement of forest canopies over time (Parker, 1995). Canopy structure, defined as an organisation of leaves, twigs and branches of a stand of vegetation in space and time (Bongers, 2001; Parker, 1995), can be described in three-dimensions using a Canopy Height Model (CHM), which is typically a raster surface representing canopy height. A CHM is thus a spatially explicit description of canopy structure over a given area of forest and is generally obtained by calculating the difference between the elevations of the canopy surface (given by a Digital Surface Models, DSM) and the underlying terrain (Digital Terrain Model, DTM). Ground-based techniques like using graduated height sticks (Fujita et al., 2003), spatial analysis of stem-mapped point data (Larson & Franklin, 2006; Song et al., 2004), hemi-spherical photography combined with stem maps (Silbernagel & Moeur, 2001; Valverde & Silvertown, 1991), and aerial photography combined with ground measurements of elevation at regular intervals (D'Aoust et al., 2004; Fujita et al., 2003; Tanaka & Nakashizuka, 1997) have been used to study forest disturbance and their consequences on canopy structure and composition over time by constructing CHMs. Ground methods are costly and tedious, often inaccurate due to the difficulty of GPS positioning in forest environments, and cannot be used extensively. The quality of CHMs and of the gap delineation derived through the analysis of aerial photographs is affected by image texture and contrast, sun-incidence angles during image acquisition, resolution, but most importantly by the accuracy of ground elevation measurements. Assessing ground elevation is critical for determining canopy height but remains very difficult when performed photogrammetrically on aerial images acquired over closed canopies (St-Onge et al., 2004). Various studies using aerial photography noted its unreliability in detecting smaller (<100 m^2) and deeper gaps (Betts et al., 2005; Fujita et al., 2003; Miller et al., 2000; Nakashizuka et al., 1995). It was also observed that the degree of error in estimating canopy height (or gap depth) increases with higher topographic relief (Tanaka & Nakashizuka, 1997).

Recently, the use of new remote sensing technologies like scanning laser altimetry, hereafter referred to as lidar (light detection and ranging), has attracted attention in forestry and ecological studies (Hyde et al., 2006; Naesset, 2002; St-Onge et al., 2004). Lidar sensors directly measure the three-dimensional distribution of plant canopies as well as sub-canopy topography, thus providing high-resolution topographic maps and highly accurate estimates of vegetation height, cover, and canopy structure (Baltsavias, 1999; Naesset, 2004; St-Onge et al., 2004). Numerous studies have verified the capacity of lidar, using small (1 m or less) as well as large (10–25 m) diameter footprints, to measure canopy height and canopy vertical structure in a variety of forest ecosystems (e.g., Clark et al., 2004; Harding et al., 2001; Parker et al., 2001). Studies have also shown that retrieval of ground elevations by lidar is superior to that of any other means of remote sensing (Clark et al., 2004; Hodgson et al., 2003; Kraus & Pfeiffer, 1998).

Recent studies have demonstrated the potential of lidar systems in delineating canopy gaps (Koukoulas & Blackburn, 2004; St-Onge & Vepakomma, 2004; Yu et al., 2004) and could successfully overcome many of the limitations associated with conventional remote sensing methods. Koukoulas and Blackburn (2004) use a rule-based algorithm on a single-time CHM to measure gap sizes (over 50 m^2) and gap shapes. Yu et al. (2004) apply a single-tree segmentation using high density (10 returns/m^2) multi-temporal lidar data to identify individual harvested trees reliably (crown radius of over 1 m). Its applicability, however, is restricted to high density lidar data. The early results of these few studies tested on semi-natural forests and plantations (Koukoulas & Blackburn, 2004; Yu et al., 2004) are promising, but still need to be extended to more complex forest structures like old-growth mixed wood forests. St-Onge and Vepakomma (2004) reliably identified newly opened gaps of size less than 1 m^2 in mixed forests. Nevertheless, none of the studies attempt to address other ecologically important dynamic characteristics of gaps, like gap closures and gap expansions.

Gap detection and delineation of its boundaries using any technique is a complex task. A basic assumption is that the gaps are easily distinguishable from the surrounding high canopies. Various researchers, depending on the type and height of forest, have proposed a critical regeneration height (adopting either a relative difference or absolute thresholds on vegetation height) beyond which the gap is considered closed (Fujita et al., 2003; Nakashizuka et al., 1995; St-Onge & Vepakomma, 2004). Such a threshold on a single-time CHM helps in mapping gaps in the canopy at a given time. However, this approach would be ambiguous in distinguishing between gaps created due to tree falls and natural spaces (interstitial space) between tree crowns. This method would be particularly difficult in slow-growing boreal forests as many stands may not have achieved full-grown crown closure, making the canopies appear open and patchy, and because coniferous trees naturally have large inter-tree distances. Moreover, gaps could be considered to be a result of tree fall events over successive periods of time (Foster & Reiners, 1986; Runkle & Yetter, 1987) and thus gap formation rates (fraction of ground area converted to new gaps annually) determined based on a single year could lead to an overestimation of true rates.

Given the high accuracy and density of lidar returns, and given the fact that they are obtained from near-nadir angles, we hypothesize that the proportion of laser pulses reaching the gap floor should be quite high, enabling the accurate delineation and near perfect interpretation of gap geometry. A new gap of any size resulting from tree fall should create a large negative elevation difference between diachronic CHMs, while a significant height increase over time within a detected gap should indicate canopy closure. Diachronic analysis will also help in filtering out the interstitial spaces between tree crowns to

reliably estimate the turnover rates of canopy gap opening and closing that is naturally occurring in old-growth forests. Based on the sensor's characteristics and early studies, the potential to advance our knowledge on gap dynamics through multi-temporal lidar remote sensing appears very high. However, before this can be achieved the necessary fundamental methods need to be elaborated and verified.

The general objective of this study is to evaluate the feasibility of reliably mapping canopy gap opening and closure based on two small footprint lidar datasets separated by a five year interval. This is achieved by first standardizing the lidar datasets through co-registration, selecting an optimal interpolation method and grid resolution suitable for delineating small gaps, and validating the results with ground verification. We then proceed to spatially and temporally characterize gaps in terms of frequency, size and nature of the gap event. The density and rates of gap opening, gap expansion and gap closure (both lateral and vertical) are derived by differentiating recent random gaps from expanded openings and recent gap closures by crown displacement through lateral growth or by regeneration.

2. Methods

2.1. Study site

The study was conducted in a 6.0 km^2 area located within the conservation zone (79°22′ W, 48°30′ N) of the *Lake Duparquet Teaching and Research Forest*, *LDTRF*, Canada (Fig. 1). This area is part of Quebec and Ontario's Claybelt and has relatively level topography (227–335 m) interspersed with a few small hills. The climate is described as subpolar, subhumid, continental with 0.8 °C mean annual temperature, 857 mm of average precipitation, an average of 64 days of frost and 160 growing season days (Environment Canada, 1993). Stands within the LDTRF originated from different fires dating from 1760 to 1919 (Dansereau & Bergeron, 1993). Most stands are mature or over mature and reach heights of 20–25 m. Balsam fir (*Abies balsamea* L. [Mill.]) is the dominant species in mature forests and is associated with white spruce (*Picea glauca* [Moench] Voss), black spruce (*Picea mariana* [Mill] B.S.P.), white birch (*Betula paprifera* [Marsh.]) and trembling aspen (*Populus tremuloides* [Michx]). The main disturbances in this area are forest fire and spruce budworm outbreaks, while individual or group mortality, and wind throw have also been reported (Dansereau & Bergeron, 1993; Harper et al., 2002; Morin et al., 1993). Although part of the forest was selectively cut during 1920–40, much of the forest is relatively virgin and remains unaffected by human intervention (Bescond, 2002). Canopy gap delineation was conducted for the entire study area while characterization of gap dynamics was made within a 225 ha area of the 258 year old stand (originated following fire in 1760).

2.2. Lidar data acquisition

The study site was surveyed on June 28th 1998 and August 14 to 16, 2003, determining an interval of approximately five growing seasons (Fig. 1). The 1998 survey was carried out using an Optech ALTM1020, a single return lidar system, at an altitude of 700 m. Because this lidar could not record both first and last returns in one pass, and had a low impulse frequency, two passes for each flight line were made to acquire the first returns, and a

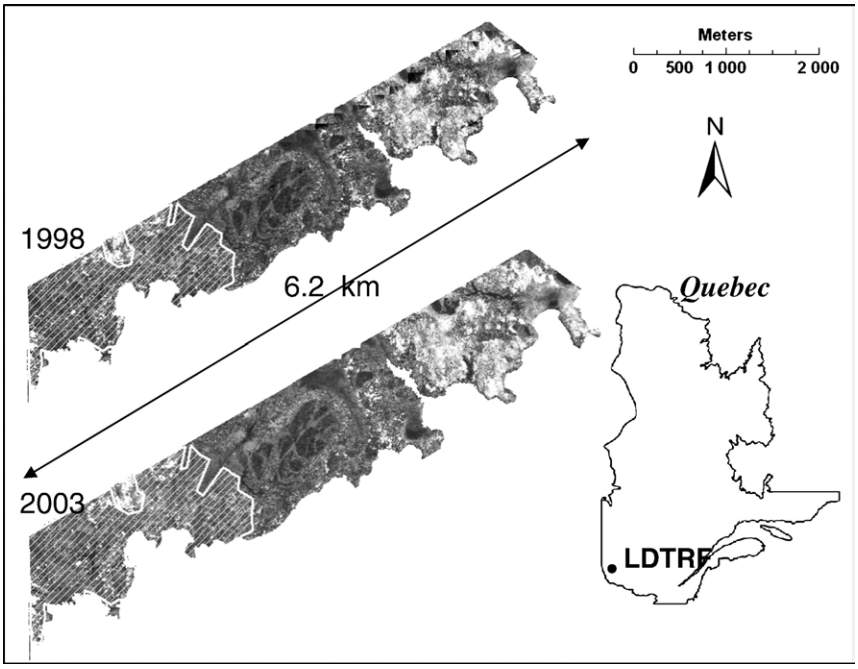

Fig. 1. Location of the Lake Duparquet Teaching and Research Forest (LDTRF), Quebec and lidar coverage in 1998 and 2003. Hashed polygons indicate the areas where complete analysis was performed.

third one was flown for the last returns. The overlap between adjacent swaths was minimal, resulting in some small data lacunae in the first returns. The data was registered to ground profiles surveyed with a high grade GPS and tacheometer. All returns were classified by the provider as ground or non-ground using the REALM software application from Optech Inc. and were assumed correct for the study. First returns not classified as ground were used to generate a vegetation surface (DSM) while first and last returns that were classified as ground were used to generate a bare-earth model (DTM).

The 2003 survey was conducted using Optech's ALTM2050 lidar flown at 1000 m AGL, such that the first and last returns were recorded for each pulse, with a 50% overlap between adjacent swaths. The data was registered to new ground profiles. The inter-swath geometrical fit was improved using the TerraMatch algorithm by Terrasolid Ltd. (Helsinki). The last returns were classified as ground or non-ground using the Terrascan algorithm of Terrasolid. The ground-classified last returns were used to build the DTM, while the DSM was created using all first returns. Table 1 presents the key survey and lidar instrument parameters. Although the specifications of the lidar instruments used in the two surveys differed in many aspects, e.g., flight altitude, scan angle, pulse frequency, the most important difference was in terms of point density (Table 1).

Both lidar datasets were assessed for accuracy in two different studies (Coops et al., 2004; Véga & St-Onge, 2007). Clearly identifiable hardwood and softwood trees, 36 (for 1998) and 77 (for 2003) in a height range of 5.6 m–33.1 m, was field measured for maximum tree height. The relationship between field measured maximum tree height and maximum lidar height for the delineated crowns was found strong (r^2 = 0.88 and 0.86 respectively) with an RMSE of 1.8 m and 1.85 m respectively.

Table 1
Specification of the lidar data acquisition

Specification	1998	2003
Lidar	ALTM1020	ALTM2050
Power (μJ)	140	200
Flight altitude (m AGL)	700	1000
Divergence (mrad)	0.3	0.2
Footprint size at nadir (cm)	21	20
Pulse frequency (Hz)	4000	50,000
Max. scan angle (degrees)	10	15
First return density (hits/m^2)	0.3	3
Ground return density (hits/m^2)	0.03	0.19
Classification software	REALM	Terrasolid

2.3. Co-registration of the data sets

Prior to multi-temporal lidar analysis, one has to ensure that the datasets generated in two different surveys are perfectly co-registered as shifts in the *X*, *Y*, or *Z* axes would result in erroneous observations of canopy height change. Although the accuracy of lidar data is known to be very high, with errors below 30 cm for ground hits (Ahokas et al., 2003; Hodgson et al., 2003; Hodgson et al., 2004), a number of factors may affect the positional accuracy of lidar returns. These factors include the quality of the GPS configuration at the time of the survey, mounting errors, reference to ground calibration measurements, etc. (Katzenbeisser, 2003). Overall, these may lead to small systematic shifts or bias in the data. We hypothesized that there could exist a possibility that the two lidar datasets were slightly misaligned and hence verified the *XYZ* fit between them.

2.3.1. Shift in X and Y

First and ground-classified returns were interpolated with a 0.5 m resolution to produce a DTM in grid format for both years. Planimetric shifts were analysed ocularly using a number of visualization strategies (like hill shading, image transparency and swiping) applied to the DTMs and DSMs. The arithmetic difference between DTMs was computed and the resulting image was analysed for trends on sloping terrain, the assumption being that if any horizontal offset existed, it should be apparent as a pattern of negative and positive elevation differences around hills. After establishing that the planimetric shifts were negligible, we measured the average altimetric shift (*Z*-shift).

2.3.2. Shift in Z

Visual analysis of the DTM difference image indicated a possible shift in *Z*. To quantify and assess this shift, various statistical moments and percentiles were generated using (1) all the corresponding ground returns for 2003 falling within a 10 cm radius of the 1998 hits (matched pairs) and (2) all ground returns within a few rare patches of bare ground. Following these comparisons, the elevation of all the 1998 returns (both vegetation and ground) was lowered to remove the estimated bias (average altimetric difference) observed between 1998 and 2003 ground returns, using the 2003 data as a reference. Subsequently, we merged the 2003 and the adjusted 1998 ground returns to maximise the overall ground density.

2.4. Generation of surface models for gap delineation

Theoretically, the quality of gaps derived from lidar should be influenced by the acquisition system (laser instrument, INS and GPS), survey characteristics (point density, flight altitude, scan angle) and interpolation errors. Decomposing the observed elevation error in the lidar data that reflected from brush/low trees, Hodgson and Bresnahan (2004) found that lidar system errors were dominant (RMSE of 21.3 cm) followed by interpolation error (RMSE of 12.8 cm). System errors can be removed by strip adjustment or error modeling. Furthermore, interpolation of point clouds onto regular grids is a common technique adopted for surface visualization and subsequent extraction of features. Although lidar allows elevation sampling at remarkably high densities, rasterization using elevation data entails a certain amount of uncertainty (Anderson et al., 2005; Lloyd & Atkinson, 2002; Mitasova et al., 2005). The level of uncertainty varies with the interpolation method adopted and so does the accuracy of gap delineation.

Researchers have noted that the magnitude of predicted (interpolation) error has a strong spatial dependence with the greatest error occurring on feature edges (for e.g., Smith et al., 2005). By deriving predicted error, e at each point (x,y), as the

difference between the raw lidar height value $Z(x,y)$ and the interpolated lidar height value $Z'(x,y)$ for that location, given as:

$$e(x,y) = Z(x,y) - Z'(x,y) \quad (1)$$

we also observed a similar trend following preliminary tests. Points well within the canopy area had the lowest prediction error ($e<1$ m), while the edges of the crowns located on the periphery of gaps had larger predicted errors ($e>1$ m). The choice of grid resolution also has a strong influence on the errors introduced during interpolation and, consequently, on gap delineation. Previous studies suggested that the optimal grid spacing should be close to the original data point spacing with nearest neighbour, TIN (Behan, 2000) and bilinear (Smith et al., 2005) interpolation techniques for urban applications. Besides, more points in each grid cell would lead to information loss while a smaller grid cell resolution would have more interpolated grid cells. For these reasons, in the context of reliable delineation of canopy gaps we have sought to identify the optimal combination of interpolation method and grid resolution for the DTM (with merged ground returns) and DSMs of both datasets.

The assessment and comparison of interpolation methods were carried out through cross-validation. Cross-validation is a standard validation technique used to identify an accurate surface interpolation algorithm where each measured point is removed and compared to the predicted value location using the remaining data points (Goovaerts, 1997). The prediction errors (e) were plotted against their measured values to observe the distribution graphically and in relation to the interpolated surfaces. In this study, an interpolation method was considered optimal when the Root Mean Square error (RMSE) of its predictions was minimum and the mode of the prediction error distribution was close to zero, specifically within the interval [−1, 1]. RMSE being a global measure of deviation, as a more robust measure we also check the mode of the prediction error distribution.

Three test windows of approximately 200 m × 200 m representing different site and vegetation characteristics commonly found at the LDTRF were used for selecting the optimal interpolator and grid resolution, namely, low dense vegetation on undulating terrain (A), high and dense vegetation on gentle slope (B) and vegetation (of varying densities and height) with a large number of openings on gentle slope (C). Table 2 details the summary statistics of the merged ground and two time vegetation returns for the test windows chosen.

Table 2
Descriptive statistics of the test windows extracted

Window	Density (points/m^2)	Minimum height (m)	Maximum height (m)	Mean height (m)	Standard deviation
A	0.45	244.86	308.84	284.93	18.03
	0.58	245.10	314.89	279.54	17.70
	2.74	244.83	315.13	282.49	18.17
B	0.12	239.62	264.85	255.08	6.40
	0.31	240.17	286.89	264.78	10.04
	1.55	240.34	287.34	267.34	9.81
C	0.27	229.85	266.19	254.68	7.10
	0.42	230.86	280.16	259.60	7.90
	4.21	229.98	281.32	262.20	7.79

Cell vales indicate statistics of the merged ground (top), 1998 first (middle) and 2003 first (bottom) returns.

2.4.1. Selection of an optimal interpolation scheme

Data exploration and quantile–quantile plots of the three windows were first used to verify that the data met the assumption of normality (Table 2). We tested eight interpolation methods representing deterministic and exact interpolators (inverse distance weighted [IDW], completely regularised splines [CRS], thin plate splines [TP], splines with tension [ST], inverse quadratic [IQ]), deterministic and inexact interpolators (local polynomial [LP]) and a geostatistical interpolator (ordinary kriging [OK]) using the Geostatistical Analyst tool of ArcGIS v9.1 (Environmental System Research Institute, Redlands, CA). Though triangulated irregular networks (TIN) are considered to retain raw values at sample locations and substantially have less error into the surface model, the process of converting TIN into a gridded surface may modify the original lidar return values. This was also observed in our data during preliminary tests and hence TIN was considered unsuitable.

The size and shape of the search neighbourhood, or the number of points to be included determine how far and where to look for measured values used in prediction. We set a maximum of 10 measured points within a circular neighbourhood of radius 1 m. The algorithms within Geospatial Analyst determined the optimal power (which was 2 for all windows and interpolators) by minimising the RMSE.

2.4.2. Selection of an optimal grid resolution

After establishing an optimal interpolator, the optimisation of grid resolution was based on two criteria, (1) to retain maximum number of laser returns in the interpolated grid i.e. minimise the loss of original lidar points in the individual surfaces (DSMs and DTM) generated for each of the test windows and (2) to minimise the number of spurious gaps delineated from the resulting CHMs. For this, first we generated, for each of the lidar datasets, several surface grids with varying grid resolutions (0.1, 0.2, 0.25, 0.5, 0.75 and 1 m) using the optimal interpolator, and compared the percentage of grid cells that had greater than one point per grid cell. Subsequently, we mapped all the new gaps for the surfaces of varying resolutions in each of the windows using the method for delineating new gaps with lidar CHMs (discussed in Sections 2.5 and 2.8). Frequency distribution of new gaps and proportionate frequency of spurious new gaps in different resolutions were generated. A minimum grid resolution beyond which the percentage grid cells with more than one point considerably higher is regarded optimal in minimising the loss of lidar points. Similarly, a matching minimum resolution beyond which the percentage spurious gaps increase greatly is considered optimal for reliable gap delineation.

2.4.3. Generation of the surface models

The DTM of the merged ground returns was generated by taking the lowest ground point within each grid cell and filling the empty cells with the interpolated ground elevation obtained using the IDW algorithm. Selection of the lowest return reduces

the risk of including lidar pulses that reflected from low vegetation but were misclassified as ground returns.

Similarly, the 2003 DSM was created by taking the highest point within each grid cell and supplementing the missing values with interpolated vegetation heights obtained using the IDW algorithm. This eliminated a large number of points that penetrated through the crown while otherwise preserving the original value of the lidar returns. However, due to the low density of points, the 1998 DSM was generated using the (exact) optimal interpolator alone. All the surfaces were generated with 0.25 m resolution within ArcGIS v.9.1. Subtracting the elevations of the merged DTM from the 1998 and 2003 DSMs respectively we created the canopy height models (CHMs) for these two years.

2.5. Gap delineation

In this study, a gap is considered as an opening in the canopy caused by the fall of a single or a group of trees of a certain height. Based on field knowledge (and also verified by Daniel Kneeshaw, personal communication) we chose 5 m as the height threshold below which areas would be identified as opening in the canopy, and above which the canopy would be considered closed. The edge of the gap is defined as the vertical projection of the canopy of trees adjacent to the gap. Open-ended systems like bare stream valleys, rock outcrops or marsh lands are not considered to be canopy gaps.

Formally, a gap indicator function G was defined for a given grid cell at (x,y) on the CHM_i as:

$$G_i(x,y) = \begin{cases} 1 & \text{if } \mathrm{CHM}_i(x,y) < a \\ 0 & \text{otherwise} \end{cases} \quad (2)$$

where $a = 5$ m in this study, $\mathrm{CHM}_i(x,y)$ is the lidar height of the canopy surface in the ith year, (x,y) is a cell that does not belong to any open-ended system. A region growing algorithm was then applied to the resulting binary grid to identify individual objects of non-null adjacent pixels. We assume that the objects smaller than 5 m^2 in size (chosen arbitrarily) could be a result of spurious low vegetation lidar returns that penetrated deep into the tree crown or that they could correspond to natural interstitial space between tree crowns. Hence they were eliminated. To further ensure that the delineated gap objects are not a result of interpolation artefacts, we set an additional condition that at least three lidar vegetation data points (returns) fall within the gap.

2.6. Accuracy assessment of gap identification using lidar

Field verification for the lidar based gap delineation was done only for the 2003 data. Given that the lidar-derived 1998 vegetation height is validated, we assume that the gaps delineated using the 1998 lidar data set and following the same procedure as described in Section 2.5, should produce similar accuracies. Despite the lower point density in 1998 this assumption is reasonable as the constraint on minimum number of lidar points and object size should eliminate spurious gap objects.

To validate the accuracy of gap identification using the 2003 lidar data, we conducted ground sampling along four randomly located line transects during September 2004. The total transect length was 980 m. A detailed visual comparison of high-resolution panchromatic Ikonos satellite data (acquired in September, 2003) and Quickbird (acquired in June, 2004) made within the 200 m buffer zone around the chosen line transects showed no apparent change in the canopy due to natural disturbances between the 2003 lidar data acquisition and the field survey.

Any opening in the canopy having an average vegetation height of less than 5 m, associated with at least 80% of its perimeter composed of high canopy trees of height greater than 10 m, was recorded as a gap. Openings belonging to open-ended systems (like rivers, trails, wetlands etc.) were not included. The

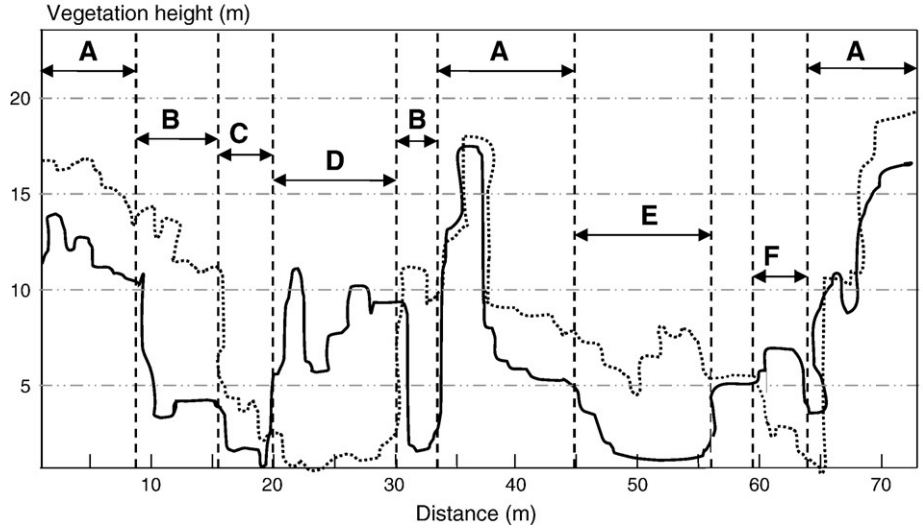

Fig. 2. Vertical profile (bold line: 1998; dotted line: 2003) along a random transect from the multi-temporal lidar CHMs showing the changes between 1998 and 2003. (A) represents a high canopy where canopy height, h, is over 5 m in both years; (B) Region where a gap present in 1998 is laterally closed by the adjacent high canopy by 2003; (C) An old gap that is still open in 2003; (D) gap expansion from an old gap; (E) gap closure from below due to regeneration; (F) random new gap.

Table 3
Comparative statistics (in meters) of the matched ground pairs

Statistic	1998	2003	Z-shift
N	916	916	
Mean	264.07	264.29	−0.22
Median	251.35	251.48	0.24
Modal	Multiple	229.86	−0.32
Minimum	228.05	228.20	−3.24
Maximum	333.10	333.40	2.02
Standard deviation	31.24	31.20	0.46

N is the total number of matched pairs; *Z*-shift is the difference in elevation of the matched pair.

initial point for each transect was fixed using a differential GPS. The transect was cruised by measuring every 5 m using a well calibrated Vertex III instrument in the set compass direction. All gaps that intersected the transect line were included in the sample. The length of the gap along each transect was measured to the closest decimeter using the Vertex III.

The accuracy assessment of the lidar delineated gaps on the CHM_{2003} was done individually for each transect by computing (i) the percentage number of gaps that were identified on lidar to the total number of gaps found on ground and (ii) the proportion of the total gap length along the transects as derived by the lidar to that of the ground measured length. Overall accuracy was assessed by considering the individual totals of columns (i) and columns (ii).

2.7. Improvement of gap geometry quantification using lidar

Deriving the exact gap geometry is fundamental for understanding and quantifying the patterns of gap disturbance (Battles et al., 1995). Gap shapes and size distributions help determine the extent of the disturbance and resource availability (Denslow & Spies, 1990; Runkle, 1985). But its measurement is often very difficult by any method. Aerial photo based methods used so far (Fujita et al., 2003; Nakashizuka et al., 1995; Tanaka & Nakashizuka, 1997) have adopted a regular grid, the smallest size being 2.5 m × 2.5 m, wherein the scale of mapping restricts the geometry of gaps resulting in either over or under-estimation. When using ground-based methods, gaps sampled along line transects are generally approximated as ellipses by measuring the longest (major) axis and the longest (minor) axis perpendicular to the major axis (Runkle, 1985; Runkle, 1992). Owing to the high density of point cloud representing the elevation and near-nadir incidence angles, we assume that the lidar-derived gaps will provide a highly reliable representation of the geometry of canopy gaps. To assess the improvement of gap geometry quantification brought about by lidar, we compared the gap size and shape of 34 lidar automatically derived gaps to their corresponding manually measured and ellipse approximations.

Area (A_l) and perimeter to area ratio (S_l) of the gap object were used for gap size and gap shape of lidar-derived gaps respectively. To replicate the ground-based measurements, we manually measured the major (a_{major}) and minor (a_{minor}) axes of each of the 34 new canopy gaps randomly selected from the lidar surface. For each of the gaps, we computed the gap area and shape approximated as an ellipse (respectively A_e and P_e) using:

$$A_e = \pi * a_{major} * a_{minor} \quad (3)$$

$$P_e = 2\pi\sqrt{\left(a_{major}^2 + a_{minor}^2\right) * (1/2)} \quad (4)$$

Differences in area (ΔA), perimeter (ΔP) and perimeter to area ratios ($\Delta P/A$) between the two methods (with lidar based estimates as a reference) were computed to quantify the gain in using lidar-derived methods.

2.8. Mapping/studying gap dynamic characteristics

Establishing that the vegetation height and gap delineation using lidar is accurate, the multi-temporal lidar analyses were extended to map other important characteristics of gap dynamics that describe the nature of the gap event, namely, area of new gap

Table 4
Estimated RMSE and distribution of error in the test windows

Interpolator	RMSE			% absolute error (<1 m)		
	A	B	C	A	B	C
Vegetation returns — 2003						
IDW	2.34	4.49	3.14	55.5	50.3	68.5
CRS	4.30	4.33	3.03	52.2	40.6	52.7
TP	2.90	19.98	13.08	53.2	40.9	65.8
ST	4.35	4.44	3.08	51.8	40.9	53.4
IQ	2.67	4.32	3.03	56.0	40.4	54.6
MQ	2.60	4.60	3.19	56.4	43.1	59.3
LP	*2.20*	*4.17*	*2.99*	54.5	43.9	51.3
OK	2.33	4.29	3.12	58.0	38.7	44.7
Vegetation returns — 1998						
IDW	3.18	5.41	4.29	50.5	33.6	33.7
CRS	3.13	5.33	*4.08*	33.9	23.7	30.7
TP	4.05	6.92	52.82	45.9	30.2	30.6
ST	3.18	5.43	4.13	37.3	31.8	28.4
IQ	3.57	5.32	*4.08*	37.1	22.7	23.8
MQ	3.37	5.74	4.30	37.0	23.5	33.6
LP	*3.03*	*5.13*	4.11	46.9	26.0	12.4
OK	3.28	5.18	4.27	38.7	23.5	31.5
Ground returns						
IDW	0.39	0.32	0.34	97.3	98.3	97.9
CRS	0.35	0.35	0.32	97.7	97.6	97.9
TP	0.39	0.39	1.31	97.0	97.5	97.6
ST	0.46	0.39	0.34	96.0	97.7	97.7
IQ	0.34	0.35	0.31	98.0	0.0	98.1
MQ	0.35	0.51	0.29	97.8	97.0	98.4
LP	0.39	*0.29*	0.34	97.5	98.9	98.3
OK	*0.33*	*0.29*	*0.28*	98.0	98.8	98.6

Numbers in italics represent minimum RMSE within a window while underlined numbers represent maximum percentage distribution of absolute error within a window.

opening, gap expansions, random gap opening, gap closures and closures from lateral and vertical growth of vegetation.

A new gap is defined as a gap in the canopy that opened between 1998 and 2003. New gaps that share the edge of a gap existing in 1998 are defined as gap expansions (see region D in Fig. 2), while the remaining new gaps are called new random gaps (see region F in Fig. 2). We define the vegetation with a height over 5 m as high canopy (see region A in Fig. 2). Gap closure occurs when an area with an average vegetation height below 5 m in 1998 increased to over 5 m during the period from 1998 to 2003. An adjacent high canopy can close a gap by crown displacement and lateral growth (see region B in Fig. 2), while the regeneration closes the gap vertically (see region E in Fig. 2).

We define G^i and G^j as the set of gap objects in the year i and year j respectively, where $i=1998$ and $j=2003$. The set of new gaps, N^{ij}, and gap closures, C^{ij}, $i<j$, were mapped using the following combinatorics on the gap objects:

$$N^{ij} = \left\{g \in G^j | g \notin O^{ij}\right\} \tag{5}$$

$$C^{ij} = \left\{g \in G^i | g \notin O^{ij}\right\} \tag{6}$$

where O^{ij} is the set of gaps that are common to both years, i.e.

$$O^{ij} = G^i \cap G^j \tag{7}$$

We defined a spurious new gap as a new gap object that has a minimum size of 5 m^2, but has fewer than 3 lidar vegetation hits in each year.

To distinguish the set of gap expansions, E^{ij}, from the set of random new gap objects, R^{ij}, we derived a buffer of 0.5 m (tolerance level sufficient to capture the differences that was fixed by trial and error), B^L, around the edge of each gap object of 1998. A buffer is a zone of specified distance around a feature. Objects that are gap expansions are then defined as:

$$E^{ij} = \left\{g \in N^{ij} | g \text{ overlaps with some element in } B^L\right\} \tag{8}$$

and the objects that are random new gaps are:

$$R^{ij} = N^{ij} \backslash E^{ij} = N^{ij} \cap \left(E^{ij}\right)^C \tag{9}$$

Similarly, deriving a buffer of 0.5 m, B^H, around the edge of each object of high canopy (canopy height over 5 m) in 1998, we define a set of objects of lateral growth, L^{ij}, $i<j$, as:

$$L^{ij} = \{g \in G^i | g \text{ overlaps with some element in } B^H \text{ and } \mathrm{CHM}_i(x,y) - \mathrm{CHM}_j(x,y) > t \forall (x,y) \in g\} \tag{10}$$

where $t=5$ m in this study.

And the set of gap objects that are vertically closing, V^{ij}, are

$$V^{ij} = C^{ij} \backslash L^{ij} = C^{ij} \cap \left(L^{ij}\right)^C \tag{11}$$

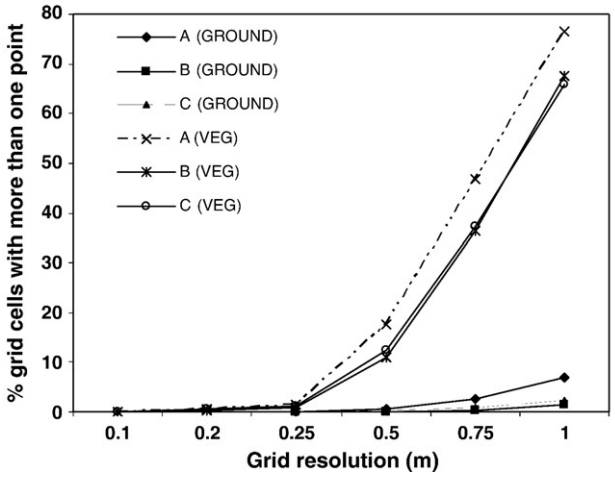

Fig. 3. Estimated percentage of grid cells having more than one lidar point in varying grid resolutions of the test windows A, B and C.

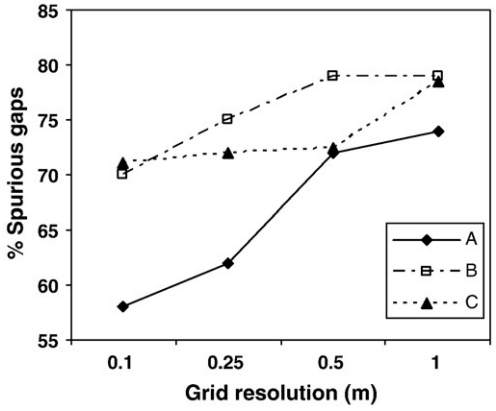

Fig. 4. Proportionate number of spurious new gaps generated from CHMs of varying grid resolutions.

2.9. Calculating gap properties

Gap size and gap perimeter were determined as the gap object area and gap object perimeter using ArcGIS. Perimeter to area ratios are used to assess gap shapes. Gap frequency i.e. the number of gaps and gap fraction i.e. proportion of land area in gaps were calculated based on the standard guidelines on forest gaps proposed by Runkle (1992). Gap size distribution, i.e. frequency of gaps in different gap size classes, are then derived.

Gap fraction for the assessment year i, GF_i, is proportion of forest area under gaps in year i, is derived using:

$$\mathrm{GF}_i = \sum_{k=1}^{M} \mathrm{AG}_k^i / aT \tag{12}$$

where AG_k^i is the area (in m^2) of the kth gap object in the ith year, a is the size of each cell and T is the total number of cells in the study area that do not belong to an open-ended system.

3. Results

3.1. Co-registration in X, Y and Z between the two lidar datasets

The analyses of the DTM difference image showed no apparent planimetric shift. If one existed, it should be negligible. Comparisons made on spots of bare ground for Z discrepancies were not conclusive. The estimated bias (average difference in Z between the corresponding ground returns in each of the two years) was 22 cm, with the 1998 data being generally higher than the 2003 data (Table 3). The estimated bias did not vary with slope. The first and last returns of the 1998 dataset were thus lowered by 22 cm.

3.2. Optimal interpolation

This investigation has shown that there is a significant variation in RMSE and individual error distribution between different interpolation algorithms (Table 4). Comparing the global characteristics, LP had the lowest RMSE among all the windows of the vegetation returns, but IDW had a similar magnitude of error with the highest mode of individual errors falling within [−1, 1] error interval (Table 4). TP had the highest interpolation errors in the vegetation returns. Among the interpolations of the last returns, OK had the smallest RMSE in all windows. However, all the interpolators had a very small magnitude of error in predicting ground elevation (Table 4). We also noted that the RMSE in interpolation of the vegetation returns has no correlation with the density of points while the percentage of points with interpolation error less than 1 m increased with the density of points.

3.3. Selection of optimal grid resolution

The loss of lidar points caused by the gridding process significantly increases with the grid resolution for all the lidar datasets. Fig. 3 shows the result of 2003 DSM and DTM. Though the point density of the 1998 first returns is slightly better than the merged ground returns, the results of the 1998 DSM are quite similar to that of the DTM. The minimum resolution for both DSMs and DTM beyond which the loss of lidar points increases significantly is 0.25 m. i.e. the loss of data points is over 18% for 2003 DSM and 4% for 1998 DSM and DTM when the grid resolution increases from 0.25 m to 0.5 m. We also note that, for all the test windows, the number of spurious new gaps increased with the increase in grid resolution (Fig. 4). As the grid resolution increases from 0.25 m to 0.5 m, there is a considerable increase in the number of spurious gaps from 58 to 75% for the window with low dense vegetation on undulating terrain (A), a steady increase for high and densely vegetated gentle slope (B) and nearly constant for vegetation with openings on gentle slope (C). Comparing the DSMs from all the test windows, we observe that the trend in increase in percentage loss of points and number of spurious gaps against increase in grid resolution did not vary with the point density (Table 2, Figs. 3 and 4). Hence, we chose 0.25 m as the optimal grid resolution for generating the lidar surfaces.

3.4. Gap delineation and accuracy assessment

Canopy gaps were automatically delineated from CHM_{2003} (Fig. 5). Fig. 6 presents an example of the matching of the automatically delineated gaps with the ground identified ones along transect-3. A comparison of the number of automatically identified gaps with the field observed ones showed a good agreement in each of the transects with respect to the number of gaps identified and the total gap length along the transect (Table 5). Overall 28 of the 29 gaps with a gap length of 309.1 m of the 423.2 m identified on the field matched the lidar-derived gaps.

Small gaps less than 5 m^2 in size were eliminated by the algorithm (for example, gaps 3 and 5 in Fig. 6 (b)). The percentage match of the total number of gaps within each transect ranged from 83.3 to 100.0 (Table 5). However, the proportion of the gap length along the transect ranged from 60.0 to 105.7% with transect-3 having the poorest match (60.0%). The overall accuracy assessed through the percentage of number of matched gaps was 96.5% and that of the matched gap length was 73.1%.

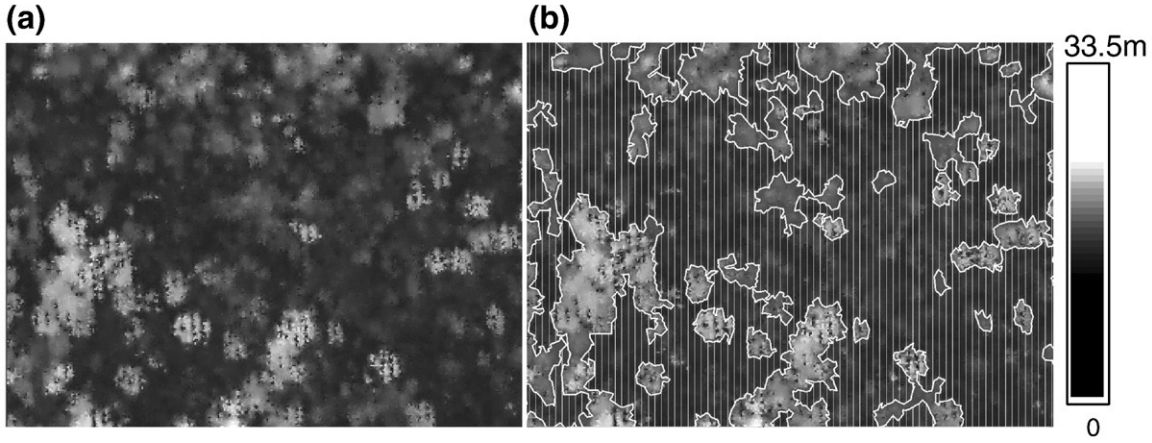

Fig. 5. An example of automatic gap detection using lidar data. (a) CHM_{2003}; (b) Delineated gaps of 2003 (polygons filled with vertical lines) overlaid on CHM_{2003}.

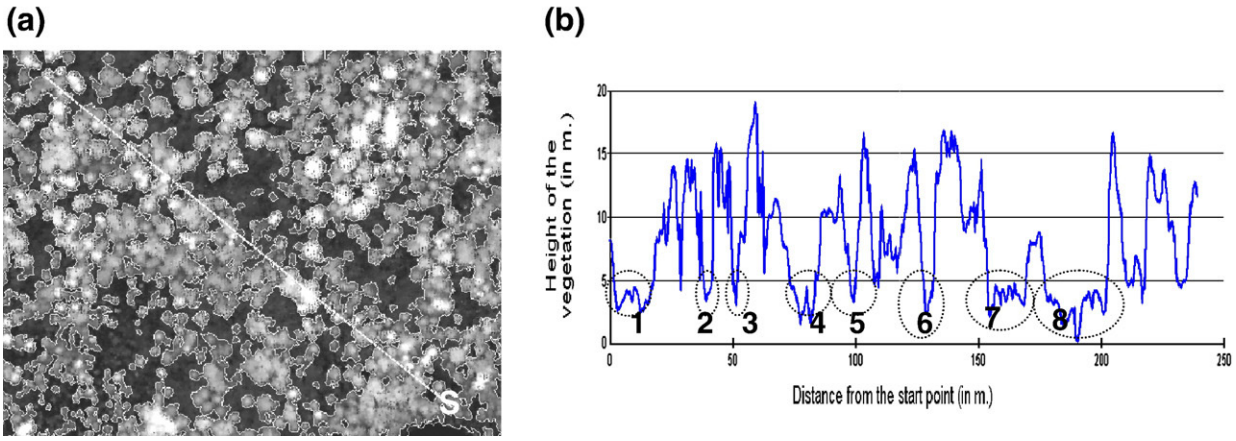

Fig. 6. A comparison of ground and lidar-derived canopy gaps; (a) Transect-3 overlaid on the CHM_{2003} along with the outline of delineated gaps, height gradation is from black (low) to white (high) on the CHM; (b) Vertical height profile from S along the transect-3. Dotted ellipses indicate possible gap regions. Gaps 3 and 5 were eliminated due to their size by the algorithm and were also not measured on the ground, and gaps 7 and 8 belonged to the same large gap but were double counted in the field.

3.5. Gain in the interpretation of gap geometry using lidar

The 34 selected canopy gaps had varying shapes with lidar *P*/*A* ranging from 0.35 to 4.16. The area of gaps extracted from the lidar CHMs (A_l) is distributed between 5.0 and 229.3 m^2 and their $perimeter_{lidar}$ between 14.2 m and 229.3 m. The area as approximated by ellipses A_e (Eq. (3)) varied between 2.0 and 523.2 m^2 while the corresponding perimeter (P_e, Eq. (4)) had values from 19.99 m to 226.54 m. On average, A_e is under or over estimated by 8 m^2 while P_e is mostly underestimated by 11.9 m when compared to the lidar-derived ones (Fig. 7 a). As a result, the perimeter to area ratio (S_l) is underestimated more often (Fig. 7 b).

3.6. Gap delineation of 1998 and 2003 lidar data

The maximum heights noted from the derived CHMs are 31.15 m and 33.50 m respectively with 2.30 m of average increase in vegetation surface height between the two years (Table 6). Every gap that has a size over 5 m^2 was mapped in the study area using the proposed method of automatic gap detection from the lidar surfaces. In all there existed 9466 and 7857 gaps in 1998 and 2003 respectively. Large gaps (over 1 ha) formed due to the impact of spruce budworm infestation in softwood dominated stands and beaver damage in hardwood dominated stands (as evidenced in field observations) were mapped. It was observed that over the 5 year study period, the total area under gaps decreased from 200.0 ha to 180.8 ha resulting in a decline of gap fraction from 0.35 to 0.31. The total gap area includes 156 ha of open area common to both years.

Table 5
Accuracy assessment of gap delineation using lidar

Transect Number	Transect length (m)	Field		Lidar		% match	
		# Gaps	Gap length (m)	# Gaps	Gap length (m)	# Gaps	Gap length (m)
1	300	7	149.96	7	158.50	100.00	105.69
2	160	8	84.99	8	78.81	100.00	92.72
3	240	6	73.01	5	71.80	83.33	98.34
4	280	8	115.20	8	69.06	100.00	59.95
Total	980	29	423.2	28	309.1	96.55	73.05

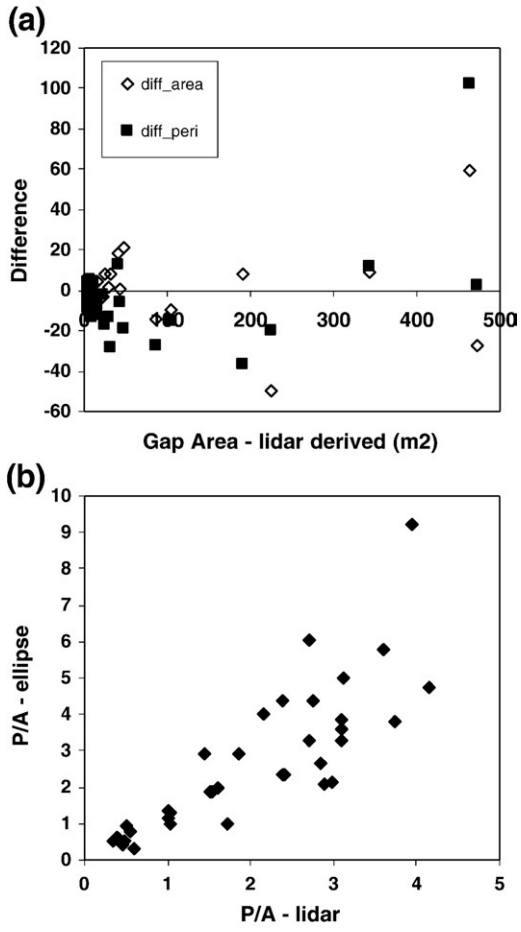

Fig. 7. Comparing gap geometry of the lidar-derived measurements to that of the ground-based ellipse approximations. (a) Difference in gap area and gap perimeter; (b) *P*/*A* ratio.

Table 6
Characteristics of the lidar-derived canopy gaps in 1998 and 2003

Statistic	1997	2003
Max. vegetation height (m)	31.15	33.50
Total number of gaps	9466	7857
Minimum gap size (m^2)	5.0	5.0
Maximum gap size (ha)	9.8	9.21
Mean gap size (m^2)	156.4	202.3
Median gap size (m^2)	19.6	24.5
Total area under gaps (ha)	200.0	180.1
Percentage frequency of gaps <100 m^2	86.7	85.1
Number of gaps of size >1 ha	23	30
Gap fraction	0.38	0.32

The common open areas consist of existing old gaps varying between 5.0 m^2 and 5.9 ha in size.

The average size of the delineated gaps is 156.4 m^2 and 202.3 m^2 respectively for 1998 and 2003. The gap size distribution in both years was consistently negative exponential with more frequent smaller gaps than larger ones. However, the gap size distribution between the two years is significant (Kolmogorov–Smirnov test, $p<0.01$). The number of gaps larger than 1 ha increased from 23 to 30, and overall the gap spatial distribution is generally more fragmented in 1998 than in 2003. Nearly 86.7% (in 1998) and 85.1% (in 2003) of the gaps have a size smaller than 100 m^2, possibly due to a single or group tree fall. The average gap perimeter significantly increased from 96.3 m to 141.8 m. The difference between the two years could to some extent be attributed to the variation in lidar point density. The perimeter to area ratio (S_l) of gaps is below 2 for 90% of 1998 gaps and 80% of the 2003 gaps, indicating that most gaps are regularly shaped.

3.7. Characterizing gap dynamics between 1998 and 2003

New gap openings and gap closures that occurred during 1998–2003 in the 225 ha area of the 258 year old stand of the study area were mapped using the combinatorics on the 1998 and 2003 gap objects as discussed in Section 2.8. The results show that old existing gaps and interstitial spaces were completely eliminated. Random new gap openings were easily discernible from gap expansions and lateral closures from regenerating gaps. Fig. 8 presents an example of the gap dynamic characteristics identified using the multi-temporal lidar analysis.

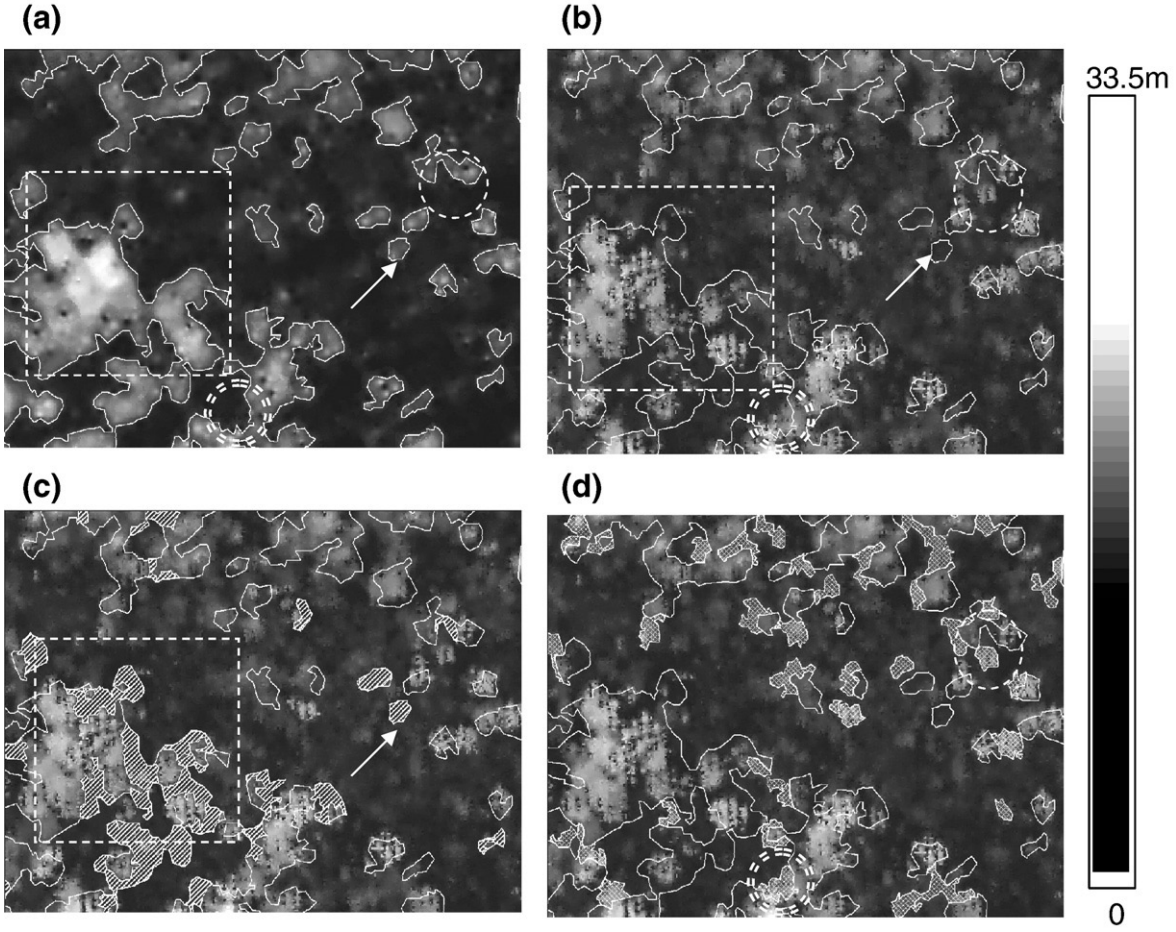

Fig. 8. Delineating new and closed gaps during 1998–2003 using lidar data. (a) Gaps in 1998 overlaid on the CHM_{1998}; (b) gaps in 1998 overlaid on CHM_{2003}; (c) identified new gaps (hashed polygons) formed by multi-tree deaths (square) and single-tree death 8.9 m^2 in size (arrow) with outline of gaps in 1998 overlaid onto the CHM_{2003}; (d) gaps (checked polygons) closed by regeneration (single dotted circle) and lateral growth of adjacent vegetation (double dotted circle) with outline of gaps in 1998 overlaid onto the CHM_{2003}.

Table 7
Characterizing gap dynamics between 1998 and 2003

Statistic	New gap opening		Gap closure	
	Random new gap	Gap expansion	Lateral closure	Regeneration
Number of gaps	1647	3107	4110	2018
Minimum gap area (m^2)	5.0	5.0	5.0	5.0
Maximum gap area (m^2)	115.6	2182.5	55.0	519.3
Average gap area (m^2)	11.4	25.8	8.1	15.8
Stdv. gap area (m^2)	7.7	64.8	65.6	20.7
Minimum gap perimeter (m)	8.66	8.74	2.24	8.60
Maximum gap perimeter(m)	148.7	1367.79	520.53	444.50
Average gap perimeter (m)	20.69	34.09	11.23	27.03
Stdv. gap perimeter (m)	10.10	43.19	9.01	20.81
% number of gaps with $P/A < 2$	48.5	70	50	78

Stdv. stands for standard deviation.

Among the 4754 new gaps that opened during the study period, 65% of them are gap expansions from the old existing gaps in 1998 (Table 7). The largest random gap opening is 115.6 m^2 while 2182.5 m^2 is the size of the largest expanded gap. The results indicate that all the new gaps are largely due to the death of one or few trees. Similarly, in this forest more gaps are seen closing from lateral growth of the adjacent matured vegetation (nearly 59%) than from the regenerating vegetation from the floor. The gap size distributions indicate that the recently closed patches are much more fragmented than the recently opened canopy gaps in this old-growth forest. The average gap size and the spread of the gap size distribution among all the classes of gap dynamics are variable (Table 7). Gap expansions and gap closures due to regeneration are much more regularly shaped than random new gaps or lateral gap closures.

4. Discussion

4.1. Optimal interpolation and grid resolution

Most studies on quantifying interpolation errors of lidar DEMs have been restricted to analysing global error patterns (using mean, standard deviation or RMSE) within bare-earth models covering urban (Mitasova et al., 2005; Smith et al., 2005) or natural environments (Anderson et al., 2005; Lloyd & Atkinson, 2002). Although seen as important and challenging in terms of discontinuities and frequent local changes in elevation, optimal interpolation for vegetation surfaces is rarely attempted, and never in studying canopy gaps. This investigation has shown that optimising grid resolution and choice of interpolation algorithm are essential, both for ground and vegetation surfaces, to ensure accurate delineation of canopy gaps.

Through an analysis of both local and global interpolation errors, our results show that there is minimal loss in accuracy in using a simpler algorithm like IDW for interpolating both vegetation and ground surfaces (Table 4). Though kriging methods provide more accurate predictions than IDW, Lloyd and Atkinson (2002) recommend IDW for data with small sample spacing, a finding later corroborated by Anderson et al. (2005). Even though local polynomial functions capture short range variation within data well; they are inexact interpolators that are not required to pass through the measured points unlike exact algorithms such as IDW. A further advantage of IDW is that it does not predict beyond maximum or minimum values. We thus chose IDW as the optimal interpolation for this data. Irrespective of the canopy structure and point density that was represented in the different test windows chosen, we also observed that a computationally less intensive algorithm like IDW is optimal for delineating gaps. Our results also indicated that interpolation error is globally not correlated with point density (Fig. 6). Comparing the mean error and RMSE, Anderson et al. (2005) noted that lidar data can withstand data reduction while maintaining accuracy of the DEM in low relief areas. Similar findings were reported by Holmgren (2004) and Maltamo et al. (2006) concerning the effect of density reduction on the accuracy of forest attribute estimates, with the exception of Magnusson (2006) who noted a significant negative effect when density was drastically reduced. Our results signify that an increase in point density helps minimise the local interpolation bias irrespective of the type of terrain and vegetation structure. Hence, we suggest that noting both the local and global patterns of the interpolation error is essential before deciding upon optimal grid resolution for a given application.

Loss of lidar points and the number of spurious new gaps increased with the grid cell size, with an optimal resolution close to the original point spacing of the 2003 lidar data, similar to the optima noted in previous studies by Behan (2000) and Smith et al. (2005) for urban applications. However, the optimal resolution chosen for the 1998 lidar dataset was much smaller than its original point spacing.

4.2. Gap delineation using lidar surface

The analysis of the 6 km^2 old-growth mixed boreal forests around lake Duparquet, Quebec, using multi-temporal lidar data gives a reliable estimate of the gap disturbance regime of these forests. Gaps of varying sizes from 5.0 to 2180.0 m^2, resulting from single to multiple tree falls, were reliably delineated. The obtained results fall within the reported characteristics of boreal forests made in earlier studies (a gap size range of 15 to 1245 m^2 as summarized for studies in boreal and subalpine forests by McCarthy, 2001). Tree mortality in old-growth boreal and subalpine forests is largely due to snapping and uprooting (McCarthy, 2001). In the study area, it was noted that tree fall may result from strong winds during violent thunderstorms, snapping under the weight of snow, and beaver activity (as evidenced by field observations and reported by Senecal et al. (2004)). The results obtained in this study support this evidence as 98% of the gaps that formed between 1998 and 2003 have a size less than 100 m^2.

An obvious advantage of this method over the rule-based algorithm using single-time CHM developed by Koukoulas and Blackburn (2004) and single-tree segmentation by Yu et al., 2004, is that canopy gaps as small as 5 m^2 were delineated

accurately. Although delineation of individual tree crowns proposed by Yu et al. (2004) could eliminate ambiguities of inter-tree spacing, its applicability and accuracy is largely restricted to high density lidar data and is potentially affected by tree crown delineation errors. Moreover, the objective of their study was to identify individually harvested trees. Koukoulas and Blackburn (2004) found the use of shrinkage and perimeter to area ratios to eliminate inter-tree spacing to be ineffective as they erroneously eliminated some canopy gaps. On the contrary, a multi-temporal data analyses of medium density lidar used in this study enabled the characterization of gaps based on the nature of their occurrence and the distinction of natural tree spacing from small canopy gaps.

The comparison of 29 field measured gaps with automatically delineated gaps on the lidar canopy height surface showed a good matching and high overall accuracy. However, as reported by many researchers, ocular gap delineation on the ground is a much more difficult task than identifying them from an aerial perspective. Large gaps are especially difficult to map on the ground and there is a chance of double counting them due to their convoluted shape. A visual overlay of transects on lidar CHMs showed that the difference that we observed in the number of gaps along transect-3 is because of double counting of a large gap that intersected the transect twice (an example of gaps 7 and 8 is seen in Fig. 6-b). Remote sensing techniques with their synoptic and wide coverage are thus definitely advantageous in such situations. Furthermore, owing to the dense point cloud acquisition and active sensors that do not rely on illumination by natural sunlight, and because of the near vertical viewing angles, lidar overcomes the limitations of most of the conventional remote sensing methods such as aerial photography.

In our field validation, the overall match of the lidar delineated total gap length with the field measured length was 73.1% of which transect-4 had the poorest match of 60.0%. This difference in the total gap length in transect-4 is largely due to the position of the transect which passes through the edge of a large gap. Deflection of a few meters from the proposed transect while cruising on the ground could possibly amount to under or over-estimating the gap length along the transect.

Gap measurement using conventional techniques is often difficult. As we noted in most studies (for example Foster & Reiners, 1986; Gagnon et al., 2004; Kneeshaw & Bergeron, 1998; Runkle, 1991), gaps are approximated to an ellipse which may not yield accurate gap geometry. In this study, using an accurate high-resolution lidar surface we were able to achieve near perfect interpretation of the gap geometry. Evaluating the gap geometry of 34 lidar-derived new gaps with their respective ellipse approximated ones, we found that the gap area was either over or underestimated and that gap perimeter was largely underestimated. The more complex the shape of the gaps with irregular perimeter, the greater was the under-estimation in gap geometry.

As hypothesized, given the nature of gaps in the study area and the capacity of lidar to detect large changes in elevation, the use of diachronic lidar data has good potential in studying gap dynamics in boreal forests. Characterizing gaps into random new gaps, gap expansions, laterally and vertically closing gaps, helps to better understand the dynamics of the boreal forests. Since the method had been verified in a complex canopy structure of open and patchy mixed boreal forests, we presume that this should be applicable to study gap dynamics in most forest ecosystem.

5. Conclusion

To the best of our knowledge, this is probably the first study to test the potential feasibility of lidar for spatially explicit mapping of boreal canopy gaps and characterizing temporal canopy gap dynamics. Ground validation shows a very high accuracy of the proposed method in delineating canopy gaps even in a complex canopy structure like that of old-growth mixed boreal forests. The results suggest that lidar is an excellent tool for efficient continuous and complete mapping of canopy gaps that are formed by single to multiple tree falls. The smallest gap that could be reliably delineated was 5 m^2 so far not achieved by any other remote sensing strategy. The use of a high-resolution DEM to identify and map forest canopy gaps has shown encouraging results, demonstrating that the proposed method has merit as a means for rapidly acquiring information on canopy structure in general, and canopy gaps in particular.

This study is also the first to propose methods to combine datasets acquired by two different sensors with dissimilar point density for ecological applications. By standardizing the two lidar data sets from different sensors we successfully analyse short-term dynamic changes in canopy gaps of boreal forests in good detail. We were able to quantify the dynamic gap characteristics in terms of size, and qualify the nature of gap events into gap expansions, random gap occurrence, gap closure due to lateral growth and gap closure due to regeneration. This should enable us to determine rates of gap formation and turnover more accurately for boreal forests.

Although a few constraints persist in using lidar owing to its higher cost of acquisition, large storage and processing complexities, need for special software packages etc., and these methods could be adopted on a sample basis to establish reliable estimates of annual rates of gap opening and closures. Recent studies propose precise and effective methods of combining lidar and multi-temporal set of aerial photos to generate retrospective time-series of canopy height models (St-Onge et al., 2007). This establishes an ample potential to extend this study to understand long-term canopy dynamics by integrating lidar with aerial photography. By exploring long-term and large-scale mortality and recruitment processes, we should be able to validate or improve our understanding of forest successional processes developed from earlier small spatial and temporal studies. Such new insights may have direct implications for forest managers who seek silvicultural and management strategies with a natural disturbance based underpinning but also have spin-offs into key areas of research like carbon sequestration in forests.

Acknowledgements

The authors wish to thank the BIOCAP Canada Foundation, the National Scientific and Engineering Research Council of

Canada and the Lake Duparquet Research and Teaching Forest, Quebec, for the financial support extended to accomplish this research.

References

Ahokas, E., Kaartinen, H., Yu, X., Hyyppä, J., & Hyyppä, H. (2003). Analyzing the effects related to the accuracy of laserscanning for digital elevation and target models. *Proceedings of the 22nd symposium of the European Association of Remote Sensing Laboratories: In Geoinformation for European wide Integration, 4–6 June 2002, Prague* (pp. 13−18)..

Anderson, E. S., Thompson, J. A., & Austin, R. E. (2005). Lidar density and linear interpolator effects on elevation estimates. *International Journal of Remote Sensing*, *26*(18), 3889−3900.

Baltsavias, E. P. (1999). Airborne laser scanning: Basic relations and formulas. *ISPRS Journal of Photogrammetry & Remote Sensing*, *54*, 199−214.

Battles, J. J., Fahey, T. J., & Harney, E. M. B. (1995). Spatial patterning in the canopy gap regime of a subalpine Abies-Picea forest in the northern United States. *Journal of Vegetation Science*, *6*, 807−814.

Behan, A. (2000). On the matching accuracy of rasterised scanning laser altimetry data.*International Archives of Photogrammetry and Remote Sensing*, *XXXIII* Amsterdam.

Bescond, H. (2002). *Reconstitution de l'historique de l'exploitation forestière sur le territoire de la forêt d'enseignement et de recherche du Lac Duparquet au cours du 20ème siècle et influence sur l'évolution des peuplements forestiers.*Mémoire de maîtrise en biologie, Université du Québec à Montréal 77 p.+ annexes.

Betts, H. D., Len, J., Brown, L. J., & Stewart, G. H. (2005). Forest canopy gap detection and characterisation by use of high-resolution Digital Elevation Models. *New Zealand Journal of Ecology*, *29*(1), 95−103.

Bongers, F. (2001). Methods to assess tropical rain forest canopy structure: An overview. *Plant Ecology*, *153*, 263−277.

Clark, M. L., Clark, D. B., & Roberts, D. A. (2004). Small foot-print lidar estimation of sub-canopy elevation and tree height in a tropical rain forest landscape. *Remote Sensing of Environment*, *91*, 68−89.

Coops, N. C., Wulder, M. A., Culvenor, D. S., & St-Onge, B. (2004). Comparison of forest attributes extracted from fine spatial resolution multispectral and lidar data. *Canadian Journal of Remote Sensing*, *30*(6), 855−866.

Dansereau, P., & Bergeron, Y. (1993). Fire history in the southern part of the boreal forest of northwestern Quebec. *Canadian Journal of Forest Research*, *23*, 25−32.

D'Aoust, V., Kneeshaw, D., & Bergeron, Y. (2004). Characterisation of canopy openness before and after a spruce budworm outbreak in the southern boreal forest. *Canadian Journal of Forest Research*, *34*, 339−353.

Denslow, J., & Spies, T. (1990). Canopy gaps in forest ecosystems: An introduction. *Canadian Journal of Forest Research*, *20*, 619.

Environment Canada (1993). *Canadian climatic normals 1961–90, Canadian Climatic Program.* Downsview, Ontario, Canada: Atmospheric Environmental Service.

Foody, G. M., Jackson, R. G., & Quine, C. P. (2003). Potential improvements in the characterisation of forest canopy gaps caused by windthrow using fine resolution multispectral data: Comparing hard and soft classification techniques. *Forest Science*, *49*(3), 444−454.

Foster, J. R., & Reiners, W. A. (1986). Size distribution and expansion of canopy gaps in a northern Appalachian spruce-fir forest. *Vegetation*, *68*, 109−114.

Fox, T. J., Knutson, M. G., & Hines, R. K. (2000). Mapping forest canopy gaps using air-photo interpretation and ground surveys. *Wildlife Society Bulletin*, *28*(4), 882−889.

Frelich, L. E., & Reich, P. B. (1995). Spatial patterns and succession in a Minnesota southern boreal forest. *Ecological Monograph*, *65*(3), 325−346.

Fujita, T., Itaya, A., Miura, M., Manabe, T., & Yamamoto, S. (2003). Canopy structure in temperate old-growth evergreen forest analyzed by using aerial photographs. *Plant Ecology*, *168*, 23−29.

Gagnon, J. L., Jokela, E., Moser, W. K., & Huber, D. A. (2004). Characteristics of gaps and natural regeneration in mature long-leaf pine flatwoods ecosystems. *Forest Ecology & Management*, *187*, 373−380.

Goovaerts, P. (1997). *Geostatistics for natural resource evaluation.* New York: Oxford University Press.

Harding, D. J., Lefsky, M. A., Parker, G. G., & Blair, B. (2001). Laser altimetry canopy height profiles: Methods and validation for closed-canopy, broad-leaved forests. *Remote Sensing of Environment*, *76*, 283−297.

Harper, K. A., Bergeron, Y., Gauthier, S., & Drapeau, P. (2002). Post fire development of canopy structure and composition in black spruce forests of Abitibi, Quebec: A landscape scale study. *Silva Fennica*, *36*, 249−263.

Hodgson, M. E., & Bresnahan, P. (2004). Accuracy of airborne Lidar-derived elevation: Empirical assessment and error budget. *Photogrammetric Engineering & Remote Sensing*, *70*(3), 331−339.

Hodgson, M. E., Jensen, J. R., Schmidt, L., Schill, S., & Davis, B. (2003). An evaluation of LIDAR- and IFSAR-derived digital elevation models in leaf-on conditions with USGS Level 1 and Level 2 DEMs. *Remote Sensing & Environment*, *84*, 295−308.

Holmgren, J. (2004). Prediction of tree height, basal area and stem volume in forest stands using airborne laser scanning. *Scandinavian Journal of Forest Research*, *19*, 543−553.

Hyde, P., Dubayah, R., Walker, W., Blair, J. B., Hofton, M., & Hunsaker, C. (2006). Mapping forest structure for wildlife habitat analysis using multi-sensor (lidar, SAR/InSAr, ETM+, Quickbird) synergy. *Remote Sensing of Environment*, *102*, 63−73.

Jackson, R. G., Foody, G. M., & Quine, C. P. (2000). Characterising windthrown gaps from fine spatial resolution remotely sensed data. *Forest Ecology & Management*, *135*, 253−260.

Katzenbeisser, R. (2003). *About the calibration of lidar sensors.* ISPRS Workshop on "3-D Reconstruction form Airborne Laser-Scanner and InSAR data"; 8–10 October 2003, Dresden.

Kneeshaw, D. D., & Bergeron, Y. (1998). Canopy characteristics and tree replacement in the southern boreal forest. *Ecology*, *79*, 783−794.

Koukoulas, S., & Blackburn, G. A. (2004). Quantifying the spatial properties of forest canopy gaps using Lidar imagery and GIS. *International Journal of Remote Sensing*, *25*(15), 3049−3071.

Kraus, K., & Pfeiffer, N. (1998). Determination of terrain models in wooded areas with airborne laser scanner data. *Photogrammetric Engineering & Remote Sensing*, *53*, 193−203.

Larson, J. A., & Franklin, F. J. (2006). Structural segregation and scales of spatial dependency in Abies amabilis forests. *Journal of Vegetation Science*, *17*, 489−498.

Lertzman, K. P., & Krebs, C. J. (1991). Gap-phase structure of subalpine old-growth forest. *Canadian Journal of Forest Research*, *21*, 1730−1741.

Lloyd, C. D., & Atkinson, P. M. (2002). Deriving DSMs from Lidar data with kriging. *International Journal of Remote Sensing*, *23*(12), 2519−2524.

Magnusson, M. (2006). Evaluation of remote sensing techniques for estimation of forest variables at stand level. Ph.D. Thesis, Swedish University of Agricultural Sciences, Umeå.

Maltamo, M., Eerikainen, K., Packalén, P., & Hyyppä, J. (2006). Estimation of stem volume using laser scanning-based canopy height metrics. *Forestry*, *79*(2), 217−229.

McCarthy, J. (2001). Gap dynamics of forest trees: With particular attention to boreal forests. *Environmental Reviews*, *9*, 1−59.

Miller, D. R., Quine, C. P., & Hadley, W. (2000). An investigation of the potential of digital photogrammetry to provide measurements of forest characteristics and abiotic damage. *Forest Ecology & Management*, *135*, 279−288.

Mitasova, H., Mitas, L., & Harmon, R. S. (2005). Simultaneous spline approximation and topographic analysis for lidar elevation data in open-source GIS. *IEEE Geoscience & Remote Sensing Letters*, *2*(4), 375−379.

Morin, H., Laprise, D., & Bergeron, Y. (1993). Chronology of spruce budworm outbreaks near Lake Duparquet, Abitibi region, Quebec. *Canadian Journal of Forest Research*, *23*, 1497−1506.

Naesset, E. (2002). Predicting forest stand characteristics with airborne scanning laser using a practical two-stage procedure and field data. *Remote Sensing of Environment*, *80*, 88−99.

Naesset, E. (2004). Effects of different flying altitudes on biophysical stand properties estimated from canopy height and density measured with a small foot-print airborne scanner. *Remote Sensing of Environment*, *91*, 243−255.

Nakashizuka, T., Katsuki, T., & Tanaka, H. (1995). Forest canopy structure analysed by using aerial photographs. *Ecological Research*, *10*, 13−18.

Parker, G. G. (1995). Structure and microclimate of forest canopies. In M. D. Lowman, & N. M. Nadkarni (Eds.), *Forest canopies* (pp. 73−106). San Diego, CA.: Academic Press.

Parker, G. G., Lefsky, M. A., & Harding, D. J. (2001). Light transmittance in forest canopies determined using airborne laser altimetry and in-canopy quantum measurements. *Remote Sensing of Environment*, *76*, 298−309.

Payette, S., Filion, L., & Delwaide, A. (1990). Disturbance regime of a cold temperate forest as deduced from tree-ring patterns: The Tantaré Ecological Reserve, Quebec. *Canadian Journal of Forest Research*, *20*, 1228−1241.

Runkle, J. (1981). Gap regeneration in some old growth forests of the eastern United States. *Ecology*, *62*, 1041−1051.

Runkle, J. R. (1985). Disturbance regimes in temperate forests. In S. T. A. Pickett, & P. S. White (Eds.), *The Ecology of Natural Disturbance and Patch Dynamics* (pp. 17−34). London: Academic Press.

Runkle, J. R. (1991). Gap dynamics of old-growth eastern forests: Management implications. *Natural Areas Journal*, *11*(1), 19−25.

Runkle, J. R. (1992). *Guidelines and sample protocol for sampling forest gaps.* General technical report, PNW-GTR-283, USDA Forest Service. Pacific Northwest Research Station, Portland, Oregon, U.S.A. 44 pp.

Runkle, J. R., & Yetter, T. C. (1987). Treefalls revisited: Gap dynamics in the south Appalachians. *Ecology*, *68*(2), 417−424.

Senecal, D., Kneeshaw, D., & Messier, C. (2004). Temporal, spatial and structural patterns of adult trembling aspen and white spruce mortality in Quebec's boreal forest. *Canadian Journal of Forest Research*, *34*, 308−316.

Silbernagel, J., & Moeur, M. (2001). Modeling canopy openness and understory gap patterns based on image analysis and mapped tree data. *Forest Ecology & Management*, *149*, 217−233.

Smith, S. L., Holland, D. A., & Longley, P. A. (2005). Quantifying interpolation errors in urban airborne laser scanning models. *Geographical Analysis*, *37*, 200−224.

Song, B., Chen, J., & Silbernagel, J. (2004). Three-dimensional canopy structure of an old-growth Douglas-fir forest. *Forest Science*, *50*(3), 376−386.

St-Onge, B., & Vepakomma, U. (2004). Assessing forest gap dynamics and growth using multi-temporal laser-scanner data. *Proceedings of the Laser-Scanners for Forest and Landscape Assessment — Instruments, Processing Methods and Applications International Conference, Frieburg im Breisgau, 3–6 Octobre 2004* (pp. 173−178)..

St-Onge, B., Jumelet, J., Cobello, M., & Véga, C. (2004). Measuring individual tree height using a combination of stereophotogrammetry and lidar. *Canadian Journal of Forest Research*, *34*, 2122−2130.

St-Onge, B., Vega, C., Fournier, R., & Hu, Y. (2007). Mapping canopy height using a combination of digital photogrammetry and airborne scanning laser altimetry. *International Journal of Remote Sensing* (accepted).

Tanaka, H., & Nakashizuka, T. (1997). Fifteen years of canopy dynamics analysed by aerial photographs in a temperate deciduous forest, Japan. *Ecology*, *78*(2), 612−620.

Valverde, T., & Silvertown, J. (1991). Canopy closure rate and forest structure. *Ecology*, *78*(5), 1555−1562.

Véga, C., & St-Onge, B. (2007). Height growth reconstruction of a boreal forest canopy over a period of 58 years using a combination of photogrammetric and lidar models. Remote Sensing of Environment (accepted).

Yu, X., Hyypae, J., Kaartinen, H., & Maltamo, M. (2004). Automatic detection of harvested trees and determination of forest growth using airborne laser scanning. *Remote Sensing of Environment*, *90*, 451−462.